Preparation and enhanced visible-light photocatalytic H_2-production activity of CdS quantum dots-sensitized $Zn_{1-x}Cd_xS$ solid solution†

Jiaguo Yu,*[a] Jun Zhang[a] and Mietek Jaroniec*[b]

Received 20th June 2010, Accepted 12th July 2010
DOI: 10.1039/c0gc00236d

CdS quantum dot (QDs)-sensitized $Zn_{1-x}Cd_xS$ solid solutions were successfully prepared by a simple cation exchange using hydrothermally synthesized ZnS nanoparticles (NPs) and $Cd(NO_3)_2$ as precursors. The prepared samples show especially high visible-light photocatalytic H_2-production activity from aqueous solutions containing Na_2SO_3 and Na_2S as sacrificial reagents even without a Pt co-catalyst. It was found that this high visible-light photocatalytic H_2-production activity is attributed to the quantum size effect of CdS; the presence of CdS QDs alters the energy levels of the conduction and valence bands in the coupled semiconductor system, which favors the electron transfer and enhances photoactivity.

Introduction

Photocatalytic hydrogen production is of great interest from both theoretical and practical viewpoints due to its possible application for converting sunlight energy into chemical energy, which is an important green chemistry issue.[1–8] Conventional TiO_2 photocatalysts possess excellent activity and stability, but require near-ultraviolet (UV) irradiation (about 4% of the solar spectrum) for effective photocatalysis, which severely limits their practical applications.[9–12] It is highly desirable to develop a photocatalyst that can use visible light effectively under sunlight irradiation. Chalcogenides are regarded as good candidates for visible-light photocatalysts. Among them, CdS is the most often applied for photocatalytic H_2-production due to its high activity under visible light and sufficiently negative flat-band potential.[13,14] However, there are still some shortcomings prohibiting its wide usage such as its photocorrosion and the need to employ noble metals as co-catalysts.[15–17] Furthermore, ZnS is another metal sulfide extensively studied for H_2 production. However, its large band gap limits the range of light effective for photocatalytic activity. Therefore, numerous efforts have been focused on doping ZnS and on the preparation of $Cd_{1-x}Zn_xS$ solid solutions in order to shift the absorption edge of ZnS into the visible light range.[18–20] It is well-known that loading of Pt on CdS or ZnS has a high hydrogen production efficiency for photocatalytic water splitting in the presence of sacrificial reagents. However, Pt is a rare and expensive noble metal. Therefore, extensive studies have been carried out to replace Pt with low-cost metals or to eliminate the usage of co-catalysts.[15–17]

Herein, we report for the first time the preparation of CdS quantum dot (QDs)-sensitized $Zn_{1-x}Cd_xS$ solid solutions for photocatalytic H_2 production using Na_2S and Na_2SO_3 as sacrificial agents under visible light. It is shown that the activity of $Zn_{1-x}Cd_xS$ is significantly enhanced due to the quantum size effect of CdS QDs even without using any noble metals as co-catalysts.

Results and discussion

Fig. 1 shows a comparison of UV-visible diffuse absorption spectra of a series of Zn- and Cd-containing sulfides (samples 1–8) with increasing Cd/Zn atomic ratio and their corresponding colors. In comparison to the absorption spectra of sample 1 (ZnS), the spectrum of sample 2 (Cd/Zn = 2.5) shifts noticeably towards higher wavelengths, implying that this sample is not a simple mixture of ZnS and CdS, but $Zn_{1-x}Cd_xS$ solid solution. Surprisingly, samples 3 and 4 with Cd/Zn ratios = 5 and 10, respectively, exhibit two absorption steps, suggesting that these samples contain two semiconductors, $Zn_{1-x}Cd_xS$ and CdS. This mixed composition can be easily explained by the difficulty of

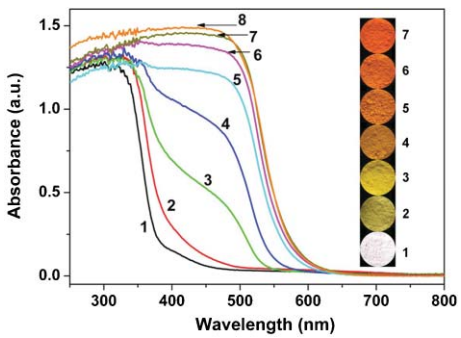

Fig. 1 UV-vis absorption spectra of ZnS (sample 1), $Zn_{1-x}Cd_xS$ (sample 2), CdS QDs-sensitized $Zn_{1-x}Cd_xS$ solid solutions (samples 3–7 with Cd/Zn ratios = 5, 10, 20, 50 and 80, respectively) and CdS NPs (sample 8) prepared at 140 °C for 12 h. The inset shows colors of samples 1–7.

[a]*State Key Laboratory of Advanced Technology for Material Synthesis and Processing, Wuhan University of Technology, Luoshi Road 122#, Wuhan, 430070, P. R. China. E-mail: jiaguoyu@yahoo.com; Fax: +86 27-87879468; Tel: +86 27-87871029*
[b]*Department of Chemistry, Kent State University, Kent, Ohio, 44242, USA, jaroniec@kent.edu; Fax: +1 330-672-3816; Tel: +1 330-672- 3790*

† Electronic supplementary information (ESI) available: Nitrogen adsorption–desorption isotherms for ZnS and CdS QDs-sensitized $Zn_{1-x}Cd_xS$ solid solutions and electron dispersive X-ray (EDX) spectrum for $Zn_{1-x}Cd_xS$ solid solution with CdS quantum dots. See DOI: 10.1039/c0gc00236d

Table 1 Experimental conditions for preparation of the samples and their physical properties

No.	*R*	Cd (at.%) (ICP-AES)	Grain size/nm	S_{BET}/m^2 g^{-1}	Band gap/eV
1	0	0	14.3 (ZnS)	38.9	3.4 (ZnS)
2	2.5	1.3	12.2 ($Zn_{1-x}Cd_xS$)	31.2	3.22 ($Zn_{1-x}Cd_xS$)
3	5	2.6	4.5 (CdS)	27.4	2.36 (CdS)
4	10	5.8	7.2 (CdS)	22.4	2.25 (CdS)
5	20	9.7	13.6 (CdS)	15.2	2.21 (CdS)
6	50	27.1	14.7 (CdS)	14.7	2.16 (CdS)
7	80	41.1	15.9 (CdS)	10.0	2.14 (CdS)
8	CdS	—	16.1 (CdS)	9.1	2.14 (CdS)

incorporation of Cd^{2+} into interstitial sites of the ZnS lattice because the radius of Cd^{2+} (0.97 Å) is much larger than that of Zn^{2+} (0.74 Å). Therefore, an increase in the Cd/Zn ratio causes separation of CdS from $Zn_{1-x}Cd_xS$ and its deposit on the surface. Consequently, it is not surprising that the absorption spectra of samples 3 and 4 exhibit two absorption steps. The direct band gaps of the samples were determined according to the Kubelka–Munk method[21–23] and their values are listed in Table 1. The large blue shifts for CdS indicate the presence of a strong quantum confinement effect in samples 3 and 4. As a result of this confinement, the band gaps of CdS QDs increase, and their redox potentials change accordingly. This issue is illustrated in Fig. 2b, which shows the redox potentials of ZnS, $Zn_{1-x}Cd_xS$ and CdS in the case of the bulk phase and quantum sizes in relation to the normal hydrogen electrode potential (NHE). The appropriate alternation in the energy levels of the conduction and valence band edges assures that CdS QDs act as sensitizers,[24] which makes $Zn_{1-x}Cd_xS$ highly active under visible light.

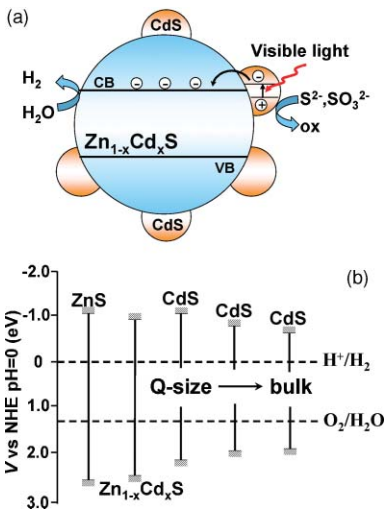

Fig. 2 (a) Schematic illustration for the charge transfer and separation in CdS QDs-sensitized $Zn_{1-x}Cd_xS$ under visible light; (b) energy levels of the conduction and valence band edges *vs.* normal hydrogen electrode (NHE, at pH = 0) for ZnS, $Zn_{1-x}Cd_xS$ and CdS with various size. (Q-size indicates that the band gap increases due to the quantum-size effect.)

The X-ray diffraction patterns (Fig. 3) indicate that the peak intensity of sample 2 (Cd/Zn ratio = 2.5) obviously becomes weak and the peak position slightly shifts to left, indicating the formation of the $Zn_{1-x}Cd_xS$ solid solution. For sample 3 (Cd/Zn ratio = 5), the diffraction peaks of CdS appear. With increasing Cd/Zn ratio, the size of CdS crystallites increases (see Table 1).

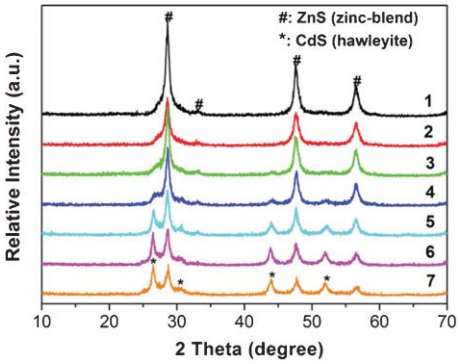

Fig. 3 XRD patterns for ZnS (sample 1), $Zn_{1-x}Cd_xS$ (sample 2), CdS QDs-sensitized $Zn_{1-x}Cd_xS$ solid solutions (samples 3–7 with Cd/Zn ratios = 5, 10, 20, 50 and 80, respectively).

The TEM image of sample 3 (Cd/Zn ratio = 5) shows that some small CdS nanocrystals (*ca.* 3–5 nm) are present on the surface of $Zn_{1-x}Cd_xS$, (which is marked by arrows on the TEM image shown in Fig. 4). The HRTEM image (inset in Fig. 4) exhibits fringes with lattice spacing of *ca.* 0.311 and 0.336 nm, which correspond to the (111) plane of cubic $Zn_{1-x}Cd_xS$ and the (111) plane of cubic CdS, respectively. This close interconnection (or heterojunction) is believed to favor the vectorial transfer of photogenerated electrons from CdS to $Zn_{1-x}Cd_xS$, thus, enhancing the charge separation and photocatalytic efficiency. The energy dispersive X-ray (EDX) spectrum shown in Figure S2 (ESI†) confirms the presence of S, Zn and Cd elements in the samples.

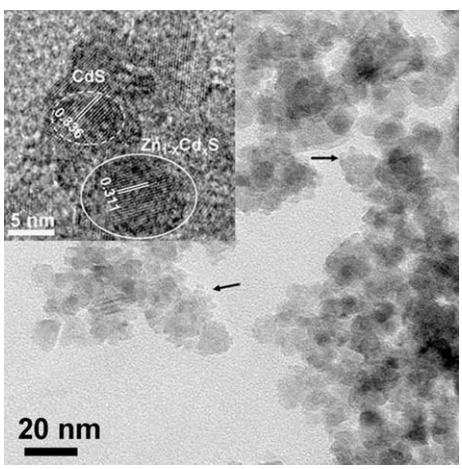

Fig. 4 TEM and HRTEM (inset) images of $Zn_{1-x}Cd_xS$ solid solution with CdS quantum dots (sample 3 obtained at Cd/Zn ratio = 5).

The visible-light photocatalytic H_2-production activity of ZnS, $Zn_{1-x}Cd_xS$, CdS QDs-sensitized $Zn_{1-x}Cd_xS$ and CdS are compared in Fig. 5. Sample 1 (pure ZnS) shows a negligible photocatalytic activity because its band gap is too large to absorb the visible light. Pure CdS (sample 8) also shows a low activity due to the absence of a co-catalyst. The loading of a small amount of CdS results in significant improvement of the photocatalytic H_2-production activity due to the formation of $Zn_{1-x}Cd_xS$ solid solution (sample 2 with Cd/Zn ratio = 2.5).

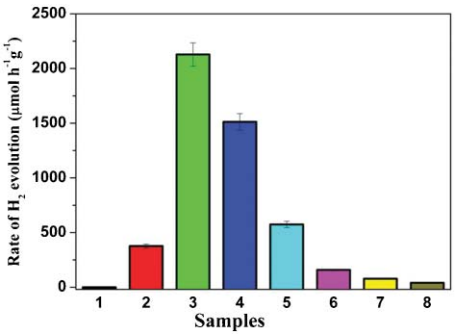

Fig. 5 Comparison of the visible-light photocatalytic H_2-production activity of ZnS (sample 1), $Zn_{1-x}Cd_xS$ (sample 2), CdS QDs-sensitized $Zn_{1-x}Cd_xS$ solid solutions (samples 3–7 with Cd/Zn ratios = 5, 10, 20, 50 and 80, respectively) and CdS NPs (sample 8) prepared at 140 °C for 12 h under visible light ($\lambda \geq 400$ nm); sacrificial solution - mixed aqueous solution containing 0.1 M Na_2S and 0.04 M Na_2SO_3; light source - 350 W Xenon arc lamp.

Usually, $Cd_{1-x}Zn_xS$ solid solution exhibits higher H_2-production activity than CdS or ZnS alone.[15–19] Surprisingly, CdS QDs-sensitized $Zn_{1-x}Cd_xS$ (sample 3 with Cd/Zn ratio = 5) shows the highest activity; its H_2-production rate is as high as 2128 μmol h^{-1} g^{-1} (which corresponds to a apparent quantum efficiency (QE) of 6.3% at 420 nm), and the rate exceeds that of CdS by more than 53 times, even much higher than that of Pt/ZnS under UV and visible light (Fig. 6). For Cd/Zn ratios > 5 the aforementioned activity decreases with increasing value of this ratio.

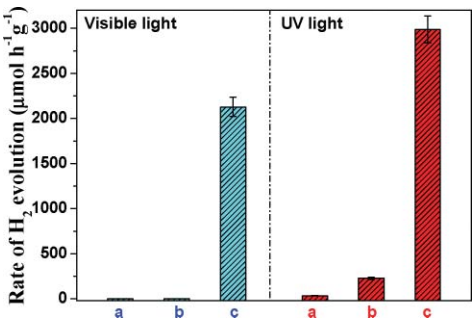

Fig. 6 Comparison of H_2-production rates of samples (a) ZnS (sample 1), (b) ZnS loaded with 1 wt% of Pt and (c) ZnS loaded with 5 mol% CdS (sample 3). The left and right panels show the photocatalytic H_2-production activity of samples under visible light ($\lambda \geq 400$ nm, 350 W Xe lamp) and UV (350 W Xe lamp) irradiation, respectively.

High H_2-production activity of samples 3 and 4 (having Cd/Zn ratios = 5 and 10, respectively) under visible light can be attributed to the electron transfer from CdS QDs to $Zn_{1-x}Cd_xS$ (see Fig. 2a). The conduction band edges of CdS QDs are deemed to be higher than that of $Zn_{1-x}Cd_xS$ due to the quantum confinement effect.[24] This facilitates the interfacial electron transfer from CdS QDs to $Zn_{1-x}Cd_xS$. Under visible light irradiation, CdS QDs are activated. The photogenerated electrons transfer from the conduction band of CdS into $Zn_{1-x}Cd_xS$ and accumulate at the lower-level conduction band of $Zn_{1-x}Cd_xS$, while holes accumulate at the valence band of CdS. Consequently, the photogenerated electron can effectively reduce H_2O (or H^+) to produce H_2. Obviously, the quantum size effects increase the band gap in CdS QDs and also shift the conduction band enough to permit transfer of photogenerated electrons. Although bulk CdS (or CdS NPs) is activated by the visible light, a low activity for samples 6 and 7 (having Cd/Zn ratios = 50 and 80, respectively) is observed. This is due to the unsuitable band position of bulk CdS. In fact, the conduction band of bulk CdS is less negative and may not allow for direct transfer of electrons from CdS to $Zn_{1-x}Cd_xS$.[6] Therefore, it is not surprising that after reaching Cd/Zn ratio = 5, its further increase causes a decrease in the specific surface area, and an increase in the size of CdS crystallites accompanied by gradual reduction of the quantum confinement effect or its disappearance, which results in a drastic decrease of the photocatalytic activity.

Conclusions

In summary, a simple cation exchange route is proposed for the fabrication of CdS QDs-sensitized $Zn_{1-x}Cd_xS$ solid solution, which shows especially high visible-light photocatalytic H_2-production activity with the rate as high as 2128 μmol h^{-1} g^{-1} (for sample 3 with Cd/Zn ratio = 5), exceeding that of CdS by more than 53 times, and being much higher than that of Pt/ZnS under UV and visible light. The corresponding apparent quantum efficiency reaches 6.3% at 420 nm even without the deposition of noble metal co-catalyst. The blue shift in the absorption spectrum confirms the quantum size effect of CdS; the presence of CdS QDs alters the energy levels of the conduction and valence bands in the coupled semiconductor system, which favors the electron transfer and enhances photoactivity. This work shows not only a possibility of using CdS QDs as a substitute for noble metals in the photocatalytic H_2 production but also presents a new method for enhancing hydrogen production activity by quantum size effect.

Experimental section

Sample preparation

All the reagents were of analytical grade and were used without further purification. Distilled water was used in all experiments. ZnS nanoparticles (NPs) were prepared by hydrothermal method using thiourea and $Zn(NO_3)_2 \cdot 6H_2O$ as precursors. In a typical synthesis, 4 mmol of $Zn(NO_3)_2 \cdot 6H_2O$ and 60 mmol of thiourea were dissolved in 80 mL of deionized water to form a clear solution after stirring for 30 min at room temperature. The mixed solution was then transferred into an autoclave with an inner Teflon lining and maintained at 140 °C for 12 h. After that, the precipitate was collected by centrifugation, washed with distilled water and ethanol three times, and then dried in an oven at 60 °C for 12 h. CdS quantum dot (QDs) sensitized-$Zn_{1-x}Cd_xS$ solid solutions were synthesized by a cation exchange and hydrothermal method using the above prepared ZnS NPs and $Cd(NO_3)_2$ as precursors. Typically, ZnS NPs (0.1 g) were ultrasonically dispersed in water, and then a certain volume of $Cd(NO_3)_2$ aqueous solution (0.01 M) was quickly added. The atomic Cd/Zn ratios = 0, 2.5, 5, 10, 20, 50, and 80 atomic% (at.%) were used to obtain a series of samples labeled from 1 to 7, respectively (see Table 1). The mixed solution volume was

adjusted to 60 mL with deionized water and stirred for 30 min at room temperature. After that, the suspension was transferred to a 100-mL teflon-lined autoclave and maintained at 140 °C for 12 h. The final products were respectively rinsed three times with distilled water and ethanol, and dried at 60 °C for 10 h. In addition, pure CdS NPs were also prepared from $Cd(NO_3)_2$ using similar procedure to that employed for the synthesis of ZnS NPs.

Characterization

X-ray diffraction (XRD) patterns were obtained on an X-ray diffractometer (type HZG41B-PC) using Cu-Kα radiation at a scan rate of 0.05° 2θ s^{-1}. The crystallite size was calculated using the Scherrer formula ($d = 0.9\lambda/B\cos\theta$, where d, λ, B and θ are crystallite size, Cu-Kα wavelength (0.15418 nm), full width at half maximum intensity (FWHM) in radians and Bragg's diffraction angle, respectively). The chemical compositions of the samples were measured by inductively coupled plasma atomic emission spectrometry (ICP-AES) using an Optima 4300 DV spectrometer (Perkin Elmer). Transmission electron microscopy (TEM) and high-resolution transmission electron microscopy (HRTEM) images were taken on a F20 S-TWIN electron microscope (Tecnai G2, Philips) linked with an Oxford Instruments X-ray analysis system using an accelerating voltage of 200 kV. The Brunauer–Emmett–Teller (BET) specific surface area (S_{BET}) of the powders was evaluated from nitrogen adsorption isotherms measured on a Micromeritics ASAP 2020 adsorption analyzer (USA); exemplary isotherms are shown in Figure S1 of the ESI.† UV-vis diffused reflectance spectra were obtained for the dry-pressed disk samples using a UV-vis spectrotometer (UV2550, Shimadzu, Japan). $BaSO_4$ was used as a reflectance standard in a UV-vis diffuse reflectance experiment.

Photocatalytic H_2-production activity

The photocatalytic hydrogen evolution experiments were performed in a 100 mL Pyrex flask at ambient temperature and atmospheric pressure, and openings of the flask were sealed with a silicone rubber septum. A 350 W Xenon arc lamp through a UV-cutoff filter (>400 nm), which was positioned 20 cm away from the reactor, was used as a visible light source to trigger the photocatalytic reaction. The focused intensity on the flask was *ca.* 180 mW cm^{-2}, which was measured by a FZ-A visible-light radiometer (made in the photoelectric instrument factory of Beijing Normal University, China) with a wavelength range of 400 to 1000 nm. In a typical photocatalytic experiment, 50 mg of catalyst was dispersed with constant stirring in an 80 mL mixed aqueous solution containing 0.1 M Na_2S and 0.04 M Na_2SO_3. Before irradiation, the system was bubbled with nitrogen for 40 min to remove air and ensure that the reaction system was under anaerobic conditions. A 0.4 mL gas was intermittently sampled through the septum, and hydrogen was analyzed by gas chromatograph (GC-14C, Shimadzu, Japan, TCD, nitrogen as a carrier gas and 5 Å molecular sieve column). All glassware was carefully rinsed with distilled water prior to use.

The apparent quantum efficiency (QE) was measured under the same photocatalytic reaction conditions. Four low-power 420 nm-LED (3 W) (Shenzhen LAMPLIC Science Co. Ltd. China), which were positioned 1 cm away from the reactor in four different directions, were used as light sources to trigger the photocatalytic reaction. The focused intensity and areas on the flask for each 420 nm-LED were *ca.* 6.0 mW cm^{-2} and 1 cm^2, respectively. The QE was calculated according to eqn (1):

$$\begin{aligned} \mathrm{QE}[\%] &= \frac{\text{number of reacted electrons}}{\text{number of incident photons}} \times 100 \\ &= \frac{\text{number of evolved } H_2 \text{ molecules} \times 2}{\text{number of incident photons}} \times 100 \end{aligned} \quad (1)$$

Acknowledgements

This work was partially supported by the National Natural Science Foundation of China (50625208, 20773097 and 20877061). This work was also financially supported by the National Basic Research Program of China (2007CB613302).

Notes and references

1 A. Fujishima and K. Honda, *Nature*, 1972, **238**, 37.
2 J. H. Park, S. Kim and A. J. Bard, *Nano Lett.*, 2006, **6**, 24.
3 Y. X. Li, Y. Z. Xie, S. Q. Peng, G. X. Lu and S. B. Li, *Chemosphere*, 2006, **63**, 1312.
4 A. Kudo and Y. Miseki, *Chem. Soc. Rev.*, 2009, **38**, 253.
5 A. J. Bard, G. M. Whitesides, R. N. Zare and F. W. McLafferty, *Acc. Chem. Res.*, 1995, **28**, 91.
6 I. Tsuji, H. Kato, H. Kobayashi and A. Kudo, *J. Am. Chem. Soc.*, 2004, **126**, 13406.
7 K. Maeda, T. Takata, M. Hara, N. Saito, Y. Inoue, H. Kobayashi and K. Domen, *J. Am. Chem. Soc.*, 2005, **127**, 8286.
8 G. K. Mor, H. E. Prakasam, O. K. Varghese, K. Shankar and C. A. Grimes, *Nano Lett.*, 2007, **7**, 2356.
9 H. G. Yang, C. H. Sun, S. Z. Qiao, J. Zou, G. Liu, S. C. Smith, H. M. Cheng and G. Q. Lu, *Nature*, 2008, **453**, 638.
10 H. G. Yang, G. Liu, S. Z. Qiao, C. H. Sun, Y. G. Jin, S. C. Smith, J. Zou, H. M. Cheng and G. Q. Lu, *J. Am. Chem. Soc.*, 2009, **131**, 4078.
11 J. G. Yu, G. P. Dai and B. B. Huang, *J. Phys. Chem. C*, 2009, **113**, 16394.
12 J. K. Zhou, L. Lv, J. Q. Yu, H. L. Li, P. Z Guo, H. Sun and X. S. Zhao, *J. Phys. Chem. C*, 2008, **112**, 5316.
13 M. Matsumura, S. Furukawa, Y. Saho and H. Tsubomura, *J. Phys. Chem.*, 1985, **89**, 1327.
14 J. F. Reber and K. Meier, *J. Phys. Chem.*, 1986, **90**, 824.
15 X. Zong, H. J. Yan, G. P. Wu, G. J. Ma, F. Y. Wen, L. Wang and C. Li, *J. Am. Chem. Soc.*, 2008, **130**, 7176.
16 L. Wang, W. Z. Wang, M. Shang, W. Z. Yin, S. M. Sun and L. Zhang, *Int. J. Hydrogen Energy*, 2010, **35**, 19.
17 C. J. Xing, Y. J. Zhang, W. Yan and L. J. Guo, *Int. J. Hydrogen Energy*, 2006, **31**, 2018.
18 K. Zhang, D. W. Jing, Q. Y. Chen and L. J. Guo, *Int. J. Hydrogen Energy*, 2010, **35**, 2048.
19 X. X. Yu, J. G. Yu, B. Cheng and B. B. Huang, *Chem.–Eur. J.*, 2009, **15**, 6731.
20 K. Zhang, D. W. Jing, C. J. Xing and L. J. Guo, *Int. J. Hydrogen Energy*, 2007, **32**, 4685.
21 N. Serpone, D. Lawless and R. Khairutdinov, *J. Phys. Chem.*, 1995, **99**, 16646.
22 E. M. Patterson, C. E. Shelden and B. H. Stockton, *Appl. Opt.*, 1977, **16**, 729.
23 J. G. Yu and X. X. Yu, *Environ. Sci. Technol.*, 2008, **42**, 4902.
24 W. K. Ho, J. C. Yu, J. Lin, J. G. Yu and P. Li, *Langmuir*, 2004, **20**, 5865.

